Author/s:
Reid, KJ;Allen, S;Tolgambayev, E

Title:
Sensitivity of Future Projections of Atmospheric Rivers Over Australia to the Choice of Thresholding Method

Date:
2025-06-16

Citation:
Reid, K. J., Allen, S. & Tolgambayev, E. (2025). Sensitivity of Future Projections of Atmospheric Rivers Over Australia to the Choice of Thresholding Method. Journal of Geophysical Research Atmospheres, 130 (11), https://doi.org/10.1029/2024JD043010.

Persistent Link:
https://hdl.handle.net/11343/362586

JGR Atmospheres

RESEARCH ARTICLE
10.1029/2024JD043010

Sensitivity of Future Projections of Atmospheric Rivers Over Australia to the Choice of Thresholding Method

Kimberley J. Reid[1,2,3], **Sophie Allen**[1,4], **and Emil Tolgambayev**[1,4]

[1]The School of Earth, Atmosphere and Environment, Monash University, Clayton, VIC, Australia, [2]Australian Research Council Centre of Excellence for Weather of the 21st Century, Melbourne, VIC, Australia, [3]School of Geography, Earth and Atmospheric Sciences, The University of Melbourne, Parkville, VIC, Australia, [4]Australian Research Council Centre of Excellence for Climate Extremes, Sydney, NSW, Australia

Key Points:

- This study assesses the sensitivity of future Atmospheric River (AR) projections to Integrated Water Vapor Transport (IVT) thresholding method over Australia
- A fixed historical IVT threshold leads to a higher frequency but weaker ARs over Australia
- The sign of the change in AR-associated precipitation can depend on the thresholding method

Supporting Information:

Supporting Information may be found in the online version of this article.

Correspondence to:

K. J. Reid,
reid.k@unimelb.edu.au

Citation:

Reid, K. J., Allen, S., & Tolgambayev, E. (2025). Sensitivity of future projections of atmospheric rivers over Australia to the choice of thresholding method. *Journal of Geophysical Research: Atmospheres*, *130*, e2024JD043010. https://doi.org/10.1029/2024JD043010

Received 20 NOV 2024
Accepted 22 MAY 2025

Author Contributions:

Conceptualization: Kimberley J. Reid
Formal analysis: Kimberley J. Reid, Sophie Allen, Emil Tolgambayev
Methodology: Kimberley J. Reid, Sophie Allen, Emil Tolgambayev
Visualization: Kimberley J. Reid
Writing – original draft: Kimberley J. Reid
Writing – review & editing: Kimberley J. Reid, Sophie Allen, Emil Tolgambayev

Abstract Atmospheric rivers (ARs) are narrow regions of strong water vapor transport in the atmosphere that can cause beneficial and hazardous hydrological impacts. One of the challenges of evaluating future AR projections is in defining future Integrated Water Vapor Transport (IVT) thresholds to use to identify ARs. The two main methods are to use a percentile of IVT based on the historical climate (fixed) or a percentile based on the future climate (relative). Although most global studies of future ARs use a fixed method, the choice of thresholding method can lead to different future projections. This study assesses the sensitivity of future projections (2080–2100) of AR frequency and precipitation impacts over Australia to the IVT thresholding method using Coupled Model Intercomparison Project 6 data under a moderate (SSP245) and high (SSP585) emissions scenario. We found that both thresholding methods lead to an increase (or no change) in AR frequency but there is considerable variation in the magnitude of the projected increase in AR frequency. Both methods suggest that heavy AR-associated precipitation will increase along with the occurrence of no rain during AR events over southeast Australia, whereas there may be a reduction in both light and heavy AR precipitation over southwest Australia. Using a fixed method leads to a drier projection for AR-associated precipitation and identifies weaker ARs. As the driest inhabited continent, understanding future precipitation and how rain-bearing weather systems, such as ARs, may change in a warmer climate is important for managing risk to Australia's future water availability.

Plain Language Summary Atmospheric rivers (ARs) are narrow regions of strong water vapor transport in the atmosphere that are important for water supply but may also cause hazardous impacts such as flooding. Understanding how ARs may change in the future is important for preparing for climate change impacts. In the present day, ARs are defined using a minimum threshold of atmospheric moisture that is based on the typical amount of atmospheric moisture we observe, and this varies by location (since the tropics are moister than the poles). But as the atmosphere warms with climate change, capacity of the atmosphere to hold moisture increases. This raises a key question about how we should define future ARs: should the minimum moisture threshold to define these extreme events be based on the future or present state of the atmosphere? Both definitions are justifiable and have benefits and limitations. In this study, we explore how the conclusions regarding future projections of ARs and AR-associated precipitation may change depending on the moisture thresholding method used. We examine ARs over Australia because this region has not been studied as much as other regions.

1. Introduction

Atmospheric rivers (ARs) are long, narrow regions of enhanced water vapor transport in the atmosphere. They are responsible for the majority of poleward water vapor transport and are an important part of the hydrological cycle (Ralph et al., 2018; Zhu & Newell, 1998). ARs can cause beneficial precipitation and are necessary for water supply in many regions (Dettinger, 2013). ARs are also associated with high impact weather events globally such as extreme rainfall, flooding, extreme winds, and landslides (Lavers et al., 2011; Ralph et al., 2006; Waliser & Guan, 2017).

ARs also occur over Australia bringing beneficial and impactful rainfall. About 20%–50% of southern Australia's wintertime rainfall is supplied by ARs occurring ahead of fronts (Reid et al., 2022). In the warmer months, ARs originating from lower latitudes can bring heavy rainfall to the northwest and east of Australia. Unusually, the strongest ARs tend to occur on the east coast of Australia (Reid et al., 2022). Another recent study found that there

is a strong correlation between ARs and heavy precipitation over Australia, especially in the east, between 1980 and 2019 (Pradhan et al., 2025).

Australian rainfall is highly variable (Nicholls et al., 1997) and 1–5 days of rainfall per year can be the difference between drought development and drought recovery (Parker & Gallant, 2022). Jin et al. (2024) showed that enhanced IVT from the Coral Sea (northeast of Australia) is a major differentiating factor between wet and dry summers and therefore drought termination. This is why small changes in the synoptic systems that bring heavy rainfall to Australia can have significant consequences for water availability.

ARs are a key driver of heavy precipitation over eastern Australia with around 30–40 of the heaviest 100 rainfall days in the agriculturally and economically significant Murray-Darling Basin (southeast Australia) being associated with ARs (Reid et al., 2022). The impacts of climate change are felt in the extremes such as changes to the behavior of drought and floods. Therefore, understanding the behavior of future extreme weather events is vital for climate change adaptation. However, future projections of extreme rainfall are highly uncertain (Pfahl et al., 2017), especially over East Australia where the majority of the population live (Clarke et al., 2022; King et al., 2023). Process-based analyses of extremes, such as analyzing changes in atmospheric water vapor and ARs, is a useful method for overcoming some of the uncertainty associated with modelling high impact rainfall (Lane et al., 2023; Reid et al., 2023).

Studies of future ARs often focus on North America or Europe (Dettinger, 2011; Gao et al., 2015; Lavers et al., 2013; Payne & Magnusdottir, 2015), although recently global studies (Rutz et al., 2019) and some Southern Hemisphere studies have been published (Espinoza et al., 2018; Reid, O'Brien, et al., 2021; Zhang et al., 2024). A review by Payne et al. (2020) found that AR frequency was expected to increase over the midlatitudes (from 1979–2002 to 2073–2096 under moderate and high emissions scenarios) with increases in flooding and extreme rainfall for many regions. A recent global study found increases in AR frequency over the global midlatitudes and increases in the proportion of precipitation attributable to ARs over Australia under moderate and high emissions scenarios in Coupled Model Intercomparison Project 6 (CMIP6) data (Zhang et al., 2024). Moreover, Reid, O'Brien, et al. (2021) found that high IVT events over Sydney would be about 80% more likely under a high emissions scenario.

Recently, studies have started to consider the uncertainty in future AR projections associated with using different AR detection tools (ARDTs) (O'Brien et al., 2022; Shields et al., 2023). These studies found that the variation in future projections between ARDTs can exceed the variations between models in CMIP5/6. One of the key differences between ARDTs is the thresholding method. Except for machine learning, Laplacian (McClenny et al., 2020) and topological (Muszynski et al., 2019) methods, AR detection often requires a choice of minimum IVT threshold to define an AR. For studies of the present climate, ARDTs may use an absolute threshold such as 250 kg m^{-1} s^{-1} or a relative threshold such as the 85th percentile of IVT at each gridcell. For studies of the future climate, a relative threshold is typically used; however, the baseline climatology used to determine the threshold may vary (i.e., historical baseline or temporally varying baseline).

Studies such as O'Brien et al. (2022) discuss the different projections that result from fixed and relative thresholds. However, since the thresholds are applied to different ARDTs, the threshold is not the only factor that could impact the results because other factors such as geometric criteria and how the IVT thresholds are calculated also vary. Therefore, in this study, we use an ARDT (Reid et al., 2020) with consistent geometric criteria and only vary the thresholding method used to identify ARs, to assess the sensitivity of future AR projections to thresholding method and control for other variables that could affect future AR projections.

One of the differences in future AR frequency scenarios that appears to result from the choice of thresholding method is whether AR frequency will increase everywhere or undergo a poleward shift (O'Brien et al., 2022). Therefore, AR frequency projections over southern Australia may be dependent on the thresholding method, which this study aims to assess. However, changes in planetary circulation are also a source of uncertainty in present and future rainfall changes over Australia (Grose et al., 2017; McKay et al., 2023), in particular over southern Australia where changes in the midlatitude storm-track can impact whether rain bearing weather systems make landfall (Frederiksen & Frederiksen, 2007). Therefore, this study will also examine the thermodynamic and dynamic contribution to future IVT projections.

This paper is structured as follows: we briefly evaluate the representation of IVT in the CMIP6 models; assess future changes in IVT from 1960–2014 to 2080–2100; examine AR frequency and size projections using the

Table 1
List of CMIP 6 Models Used

Reference	Model	Variable	Scenario	Ensemble member	Time period
(Bi et al., 2020)	ACCESS-CM2	hus,ua,va,pr	historical,ssp245,ssp585	r1i1p1f1	1960–2014; 2080–2100
(Ziehn et al., 2020)	ACCESS-ESM1-5	hus,ua,va,pr	historical,ssp245,ssp585	r1i1p1f1	1960–2014; 2080–2100
(Wu et al., 2019)	BCC-CSM2-MR	hus,ua,va	historical,ssp245,ssp585	r1i1p1f1	1960–2014; 2080–2100
(Swart et al., 2019)	CanESM5	hus,ua,va,pr	historical,ssp245,ssp585	r1i1p1f1	1960–2014; 2080–2100
(Lovato et al., 2022)	CMCC-ESM2	hus,ua,va,pr	historical,ssp245,ssp585	r1i1p1f1	1960–2014; 2080–2100
(Voldoire et al., 2019)	CNRM-CM6-1	hus,ua,va,pr	historical,ssp245,ssp585	r1i1p1f2	1960–2014; 2080–2100
As above	CNRM-CM6-1-HR	hus,ua,va	historical,ssp245,ssp585	r1i1p1f2	1960–2014; 2080–2100
As above	CNRM-ESM2-1	hus,ua,va,pr	historical,ssp245,ssp585	r1i1p1f2	1960–2014; 2080–2100
(Li et al., 2020)	FGOALS-g3	hus,ua,va,pr	historical,ssp245,ssp585	r1i1p1f1	1960–2014; 2080–2100
(Swapna et al., 2015)	IITM-ESM	hus,ua,va,pr	historical,ssp245,ssp585	r1i1p1f1	1960–2014; 2080–2100
(Gutjahr et al., 2019)	MPI-ESM1-2-HR	hus,ua,va,pr	historical,ssp245,ssp585	r1i1p1f1	1960–2014; 2080–2100
(Cao et al., 2018)	NESM3	hus,ua,va,pr	historical,ssp245,ssp585	r1i1p1f1	1960–2014; 2080–2100
(Seland et al., 2020)	NorESM2-LM	hus,ua,va,pr	historical,ssp245,ssp585	r1i1p1f1	1960–2014; 2080–2100

different thresholding methods and examine the thermodynamic and dynamic contribution to IVT changes; quantify AR-associated precipitation and intensity changes under different warming scenarios and IVT thresholds.

The two main goals of this study are: (a) examine projections of ARs over Australia and associated precipitation impacts, and (b) understand the sensitivity of future AR projections to the thresholding method in the AR detection algorithm and how this may affect our interpretation of future projections.

2. Data and Methods

2.1. IVT Data

We used IVT data from the European Center for Medium-Range Weather Forecasting Reanalysis (ERA5; Hersbach et al., 2020) to evaluate the climate models. Daily IVT was calculated by computing the magnitude of the eastward and northward components of vertically IVT in ERA5 from 1960 to 2014. The IVT in other common reanalyses, such as the Modern-Era Retrospective analysis for Research and Applications 2 (MERRA v2) (Gelaro et al., 2017) and the Japanese 55 year Reanalysis (JRA55) (Ebita et al., 2011), correlates well with ERA5 (Collow et al., 2022), so the choice of reanalysis is unlikely to cause significant uncertainty for this analysis.

Specific humidity and horizontal winds from 13 CMIP6 models (Table 1) were used to calculate historical (1960–2014) and future (2080–2100) daily IVT. Since Australian rainfall is highly variable (Nicholls et al., 1997), we have selected a long historical record to smooth out the interannual variability; however, we retained the commonly used future period 2080–2100 to maximize the warming signal. The proportion of months in each phase of the El Niño-Southern Oscillation was comparable for the future (2080–2100) and historical (1960–2014) periods (not shown).

Integrated Water Vapor Transport was defined as: $g^{-1}\sqrt{\left(\int_{1000}^{300} qu\,dp\right)^2 + \left(\int_{1000}^{300} qv\,dp\right)^2}$

where g is the acceleration due to gravity (ms^{-2}), q is the specific humidity in kg kg^{-1}, u and v are horizontal winds in ms^{-1} and p is pressure in Pa. All models and ERA5 data were regridded to a common $2° \times 2°$ horizontal grid using bilinear interpolation to control for varying resolutions between models. Two future climate scenarios, shared socioeconomic pathways 245 and (SSP245) and 585 (SSP585), were assessed which represent moderate and high emissions scenarios, respectively (O'Neill et al., 2016).

2.2. Thermodynamic and Dynamic IVT Scaling

The contribution of the thermodynamic and dynamic components of IVT to the total future IVT change were calculated using the scaling method introduced by Gao et al. (2015) and used by Payne et al. (2020). This method uses the ratio of the mean future and historical integrated water vapor (vertical integral of specific humidity) as a scaling factor. The scaling factor (for each emissions scenario) is multiplied by the historical IVT to calculate the thermodynamic component of future IVT. The residual of the modeled IVT and thermodynamic component of IVT is considered the dynamic component of future IVT.

2.3. Atmospheric River Identification

A modified version of the Reid ARDT (Reid et al., 2020) was used to identify ARs. An independent study by Pradhan et al. (2025) found that the Reid ARDT was one of the most effective detection algorithms for studying ARs and precipitation over Australia. The Reid ARDT identifies continuous regions of IVT that exceed a specified threshold. Geometric criteria including a minimum length, aspect ratio and centroid latitude criteria are applied to the IVT regions in order to distinguish ARs from other high IVT systems such as tropical cyclones or tropical convergences zones. Because of the coarse resolution climate model data, the AR minimum length criterion was relaxed from 2,000 to 1,500 km compared to previous versions. The minimum length of 1,500 km is used in the literature, for example, Brands et al. (2017) and Gershunov et al. (2017) and leads to a 1%–5% of time difference in AR frequency over Australia in the ERA5 historical record (not shown). A minimum aspect ratio of two was use and the AR centroid could not be within 5° latitude of the equator.

The IVT thresholding method was modified from an absolute threshold to a percentile-based relative threshold. The ERA5 and historical CMIP6 ARs were identified using an IVT threshold of the 85th percentile of IVT over the period 1960–2014 for each grid cell. This threshold was chosen because it is widely used in the literature (O'Brien et al., 2022; Rutz et al., 2019) and represents the median IVT in ARs found in observational studies by Neiman et al. (2008). The future period ARs were identified using two thresholds: a fixed and relative threshold. The fixed threshold (also described in O'Brien et al., 2022) defines the boundary of ARs as the 85th percentile IVT value based on the historical climatology. In other words, the fixed method uses the same threshold as was used to identify historical ARs and is only relative in space. The relative method defines the boundary of ARs as the 85th percentile IVT value based on the future period (i.e., the 85th percentile of daily IVT using all days between 2080 and 2100). For simplicity, ARs identified using historical IVT to define the thresholds will be referred to as "fixed threshold" and ARs identified using future IVT to define the thresholds will be referred to as "relative threshold." The historical ARs are defined using the 85th percentile of IVT over the historical period.

AR-associated precipitation is defined as precipitation that occurred in a gridbox that was deemed to contain an AR on the same day. Note that CNRM-CM6-1-HR was missing some precipitation data and was excluded from this analysis.

3. Model Evaluation

Since CMIP6 IVT has been widely examined in the literature already, we present a brief model evaluation.

The climatological mean and variability of IVT are broadly captured in the multimodel mean (MMM). The models show a slightly higher mean IVT over the east coast (Figure 1c) and more variability in the west (Figure 1d) but these differences are small.

We further examined the difference in climatological mean IVT between each model and ERA5 (Figure 2). BCC-CSM2-MR displayed large positive biases in the climatological mean IVT, so we decided to remove this model

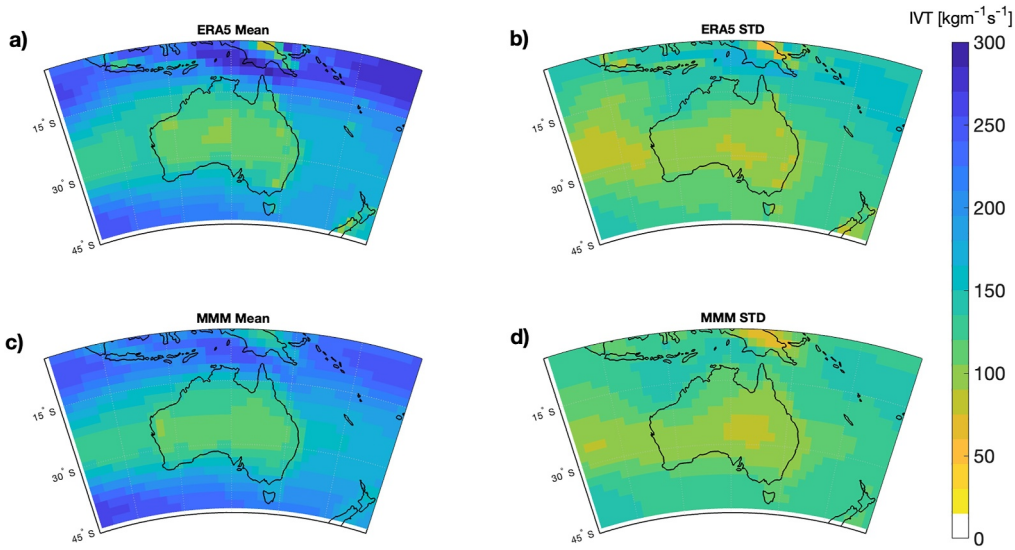

Figure 1. ERA5 and Multimodel Mean (MMM) daily (a and c) mean Integrated Water Vapor Transport, and (b and d) standard deviation for the historical period (1960–2014).

from the rest of the study. Most models have an IVT bias of less than 50 kg m^{-1} s^{-1} over Australia except NorESM2-LM which has a positive IVT bias over northern Australia of about 100 kg m^{-1} s^{-1}.

Since the mean only represents one part of the IVT distribution, we also examined the root-mean square error (RMSE) between IVT quantiles in ERA5 and each model at each grid (Figure 3). In other words, we calculated the 5th to 95th percentile of IVT (with 5 percentile increments) in ERA5 and each model and determined the RMSE between them as in Reid, O'Brien, et al. (2021).

The IVT distributions in most models are similar to ERA5 over the Australian continent except for NorESM2-LM which appears to have a positive IVT bias over northern Australia. Some models exhibit a positive IVT bias in the northwest of Australia. Although there are large RMSE values over the Maritime Continent, likely due to variable

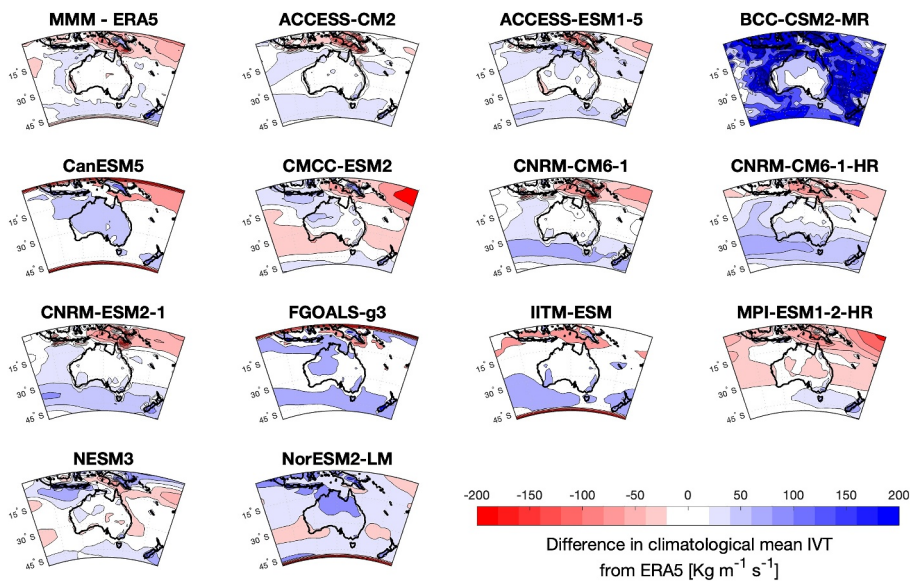

Figure 2. Difference in climatological mean Integrated Water Vapor Transport between each model and ERA5 for the historical period (1960–2014). Model names are above each subplot and MMM is the multimodel mean.

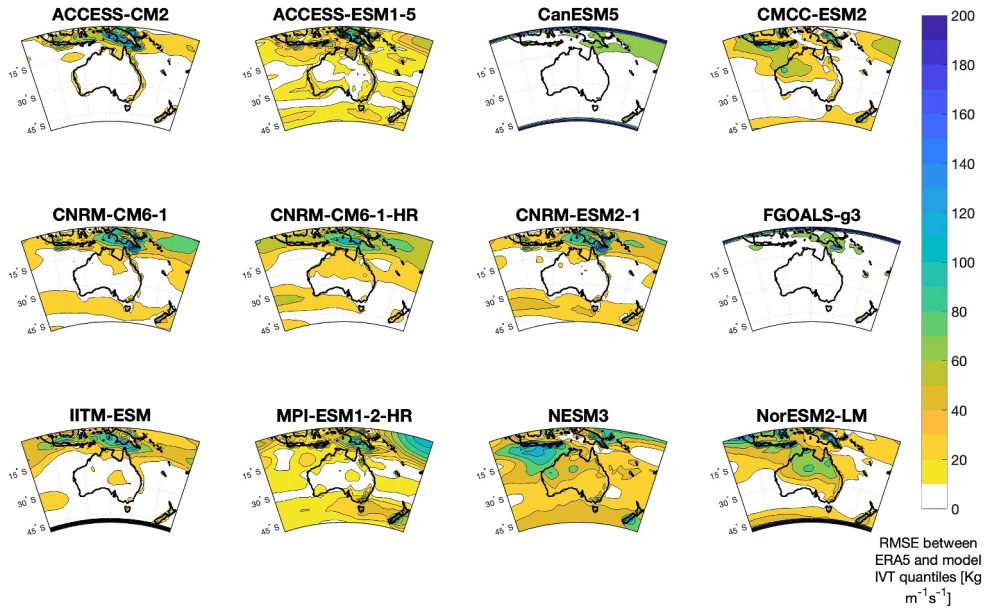

Figure 3. Root-mean square error between Integrated Water Vapor Transport (IVT) quantiles in ERA5 and each model at every grid cell. Quantiles are the 5th to 95th percentile of IVT (with 5 percentile increments).

topography not well represented in the coarse climate models, this area is not the focus of this study. Comparison of historical AR frequencies in each model and ERA5 are shown in Figure S1 in Supporting Information S1.

4. Future Projections of IVT

We now examine future projections of IVT. Figure 4 shows the projected change in the 85th percentile of IVT for each model under the SSP245 or moderate emissions scenario. Although atmospheric moisture is expected to increase in a warming world (Held & Soden, 2006) the 85th percentile of IVT over the Australian region does not increase everywhere (red colors in Figure 4). As mentioned in Section 2.3, the 85th percentile was chosen because it is a threshold commonly used to identify ARs. Previous studies have found that the mean IVT is projected to

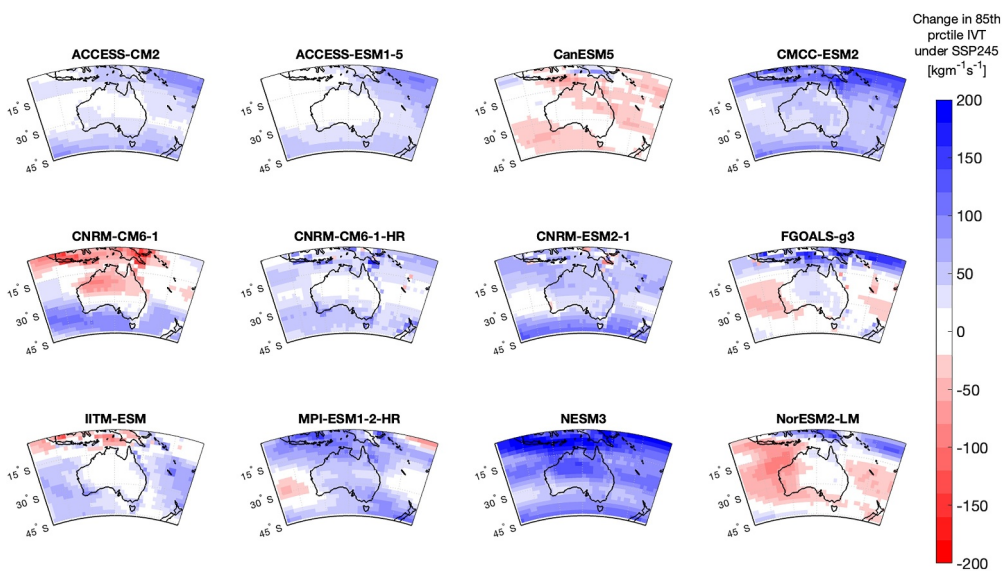

Figure 4. Change in 85th percentile Integrated Water Vapor Transport [kg m^{-1} s^{-1}] between the future (2080–2100) and historical (1960–2014) period under the SSP245 scenario. The 85th percentile was used because it is a common threshold for defining atmospheric rivers.

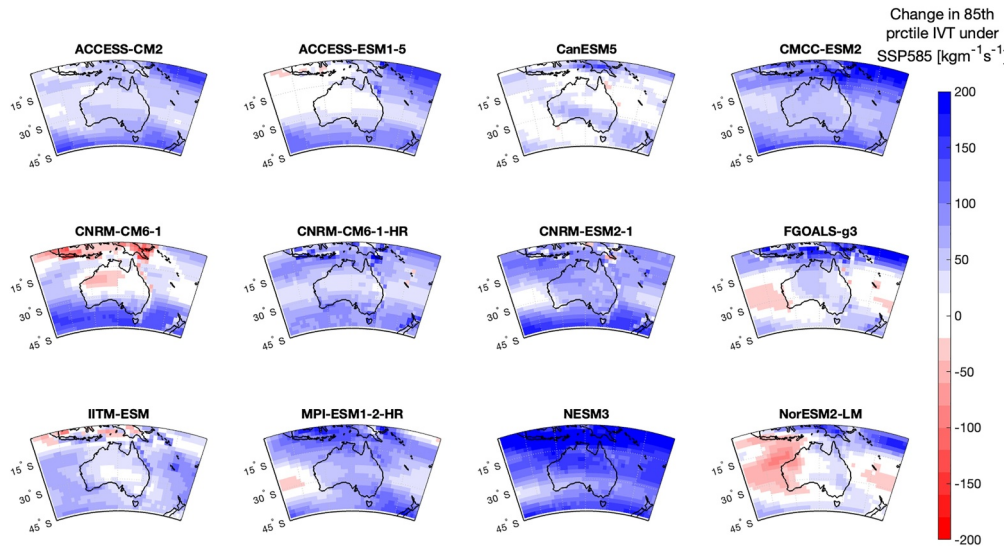

Figure 5. Change in 85th percentile Integrated Water Vapor Transport [kg m^{-1} s^{-1}] between the future (2080–2100) and historical (1960–2014) period under the SSP585 scenario.

increase everywhere according to CMIP5/6; however, the dynamic component of the mean IVT may increase or decrease in some locations while the thermodynamic change in mean IVT dominates the dynamic change (O'Brien et al., 2022).

We also examine the change in the 85th percentile of IVT under the SSP585 or high emissions scenario (Figure 5). Models that previously projected decreases in IVT under SSP245, project weaker decreases or even increases in the 85th percentile of IVT under SSP585 (e.g., CanESM5 and NorESM2-LM).

5. Future Projections of Atmospheric Rivers

O'Brien et al. (2022) found that AR detection methods that use an absolute or fixed (in time) percentile-based IVT threshold to identify ARs tended to produce an increase in AR frequency with warming, whereas methods that use a relative (in time and space) IVT threshold to identify ARs, indicated a poleward shift in AR occurrence with warming. A poleward shift in ARs may be the difference between ARs making landfall over southern Australia or not, which would have considerable implications for Australian water availability. Hence, it is vital to understand how sensitive AR projections are to the choice of method.

Therefore, the analysis of future ARs over Australia in this study used a detection algorithm with geometric criteria held constant but two thresholding methods as outlined in Section 2.3. The fixed method uses the 85th percentile of the historical IVT as the minimum boundary for an AR, whereas the relative method uses the 85th percentile of the future IVT as the minimum boundary for an AR. Figure 6 shows the projected change in AR frequency over Australia using both methods and for both SSP scenarios.

The fixed method suggests an increase in AR frequency over the Australian region. The increases in AR frequency are projected to be greater under SSP585 using the fixed threshold. We observe weaker frequency increases in the subtropics (around 25°S–30°S) possibly due to a strengthening subtropical ridge (Rudeva et al., 2019) and greater frequency increases over the Southern Ocean (south of the Australian mainland) as also noted in previous studies (Espinoza et al., 2018). In contrast, the relative method suggests much smaller increases or even no change in AR frequency at the end of the 21st century. Moreover, there is far less agreement in the direction of change as indicated by the lack of stippling. The difference in AR frequency projections is larger for different thresholding methods than for different shared socioeconomic pathways. For example, over southeast Australia, the frequency difference between the fixed and relative thresholds is about 50%–100% for SSP585 (Figures 6c and 6d). There is minimal difference in AR frequency between the two climate scenarios for the relative threshold method (Figures 6b and 6d).

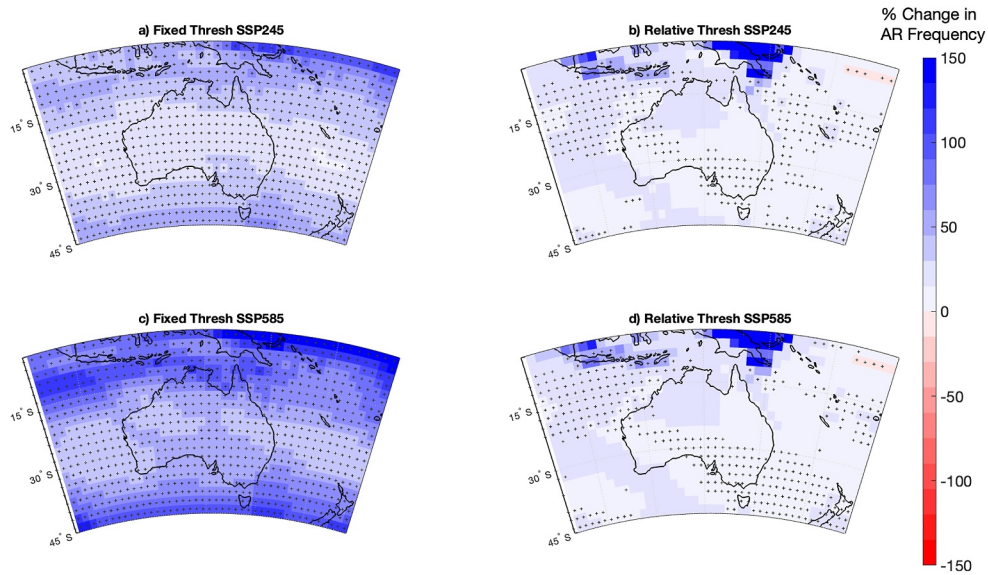

Figure 6. Multimodel mean percentage change in atmospheric river (AR) frequency (proportion of timesteps with an AR) between the future (2080–2100) and historical (1960–2014) periods using (a and c) the fixed, and (b and d) relative threshold methods. Stippling indicates where at least half of models agree on the sign of the change (and that sign is the same as the multimodel mean). Labels above the subplots indicate the thresholding method and shared socioeconomic pathway. Percentage change in frequency was calculated for each model before the multimodel mean was calculated.

We now explore some of the reasons for the difference in future AR frequency from the two thresholding methods. The fixed method identifies larger ARs, which is shown in Figure 7.

Figure 7 shows the distribution of number of gridboxes per AR under the two SSPs and two thresholding methods. The fixed method tends to identify larger ARs, whereas the relative method has a similar AR spatial size distribution to the historical period. The relative method is designed to account for changes in the background IVT, so it is not surprising that the spatial footprint is comparable to the historical period. Since the fixed threshold is often, albeit not always (i.e., Figures 4 and 5), less restrictive, it likely leads to broader ARs being identified and

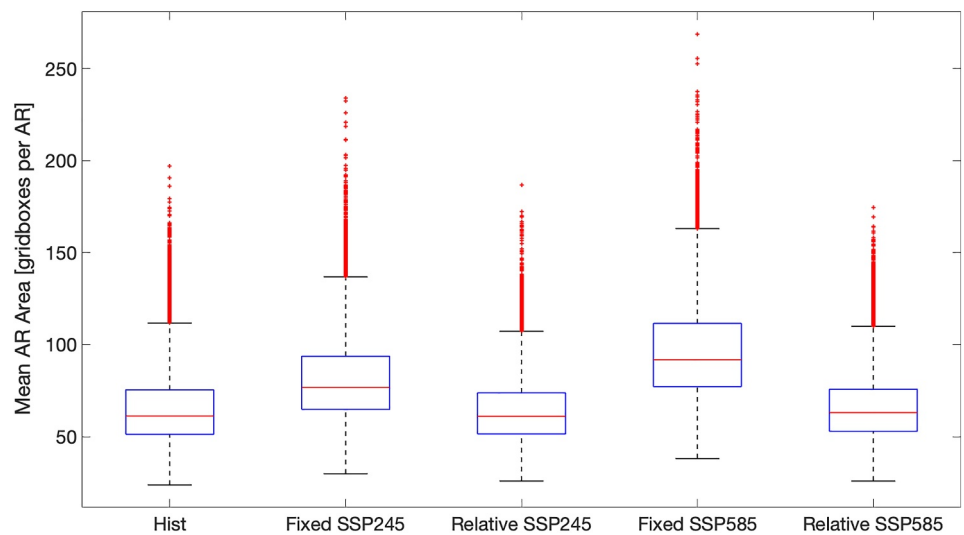

Figure 7. Box and whisker plot showing the daily multimodel mean number of gridboxes per atmospheric river identified for the historical period, both thresholding methods and both SSPs. Red horizontal line is the median, blue box shows the interquartile range, and whiskers extend to the value of median plus or minus 1.5 times the interquartile range.

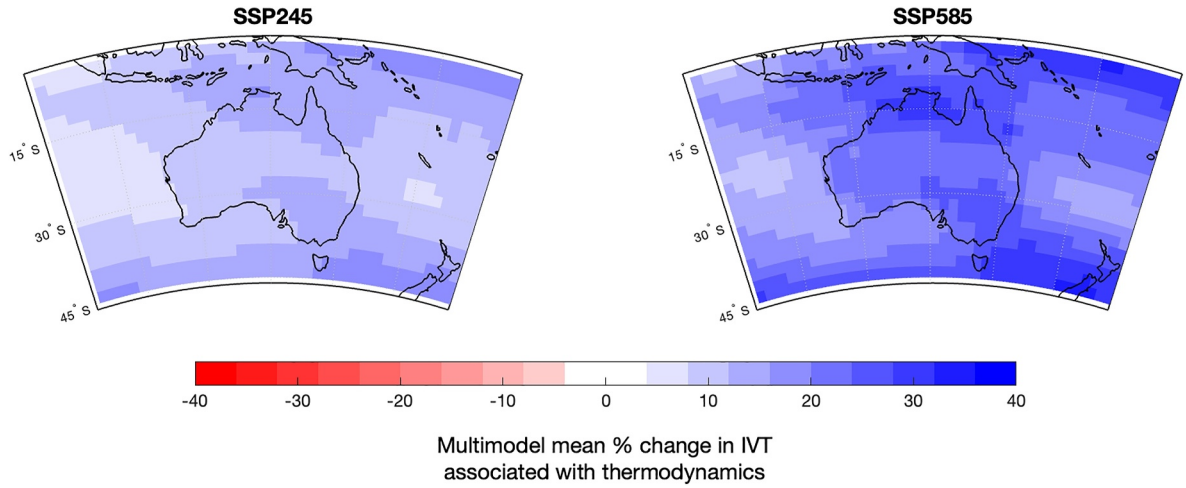

Figure 8. Following the method described in Section 2.2, multimodel mean percentage change in Integrated Water Vapor Transport relative to the historical period (1960–2014) associated with thermodynamic changes under SSP245 and SSP585.

hence the frequency of AR occurrence (when frequency is defined as the number of gridboxes or timesteps) appears larger using the fixed method.

Given the relative method is thought to emphasize dynamical changes to ARs (O'Brien et al., 2022), we assessed the thermodynamic and dynamic scaling of IVT over Australia to evaluate whether the thermodynamic and dynamic components can help to explain the differences in AR frequency that stems from the thresholding methods. Figures 8 and 9 show the multimodel mean change in IVT associated with thermodynamic and dynamic changes, respectively.

Figure 8 shows an increase in the thermodynamic component of IVT everywhere with the strongest increases in the southern Tasman Sea between Australia and New Zealand and the weakest increases near the subtropical ridge. Qualitatively, the spatial pattern of IVT increase in Figure 8 is similar to the AR frequency changes when using the fixed threshold in Figure 6.

In contrast, Figure 9 shows the IVT change associated with dynamic changes and indicates a decrease in IVT due to dynamics except at higher latitudes of the domain. We did find a weakening of westerly *u* winds over Australia at 850 hPa in most models (Figures S5 and S6 in Supporting Information S1), however, the change in the dynamic component is approximately one order of magnitude less than the change in the thermodynamic component of IVT indicating that the thermodynamic component dominates the future change in IVT. The spatial pattern of the

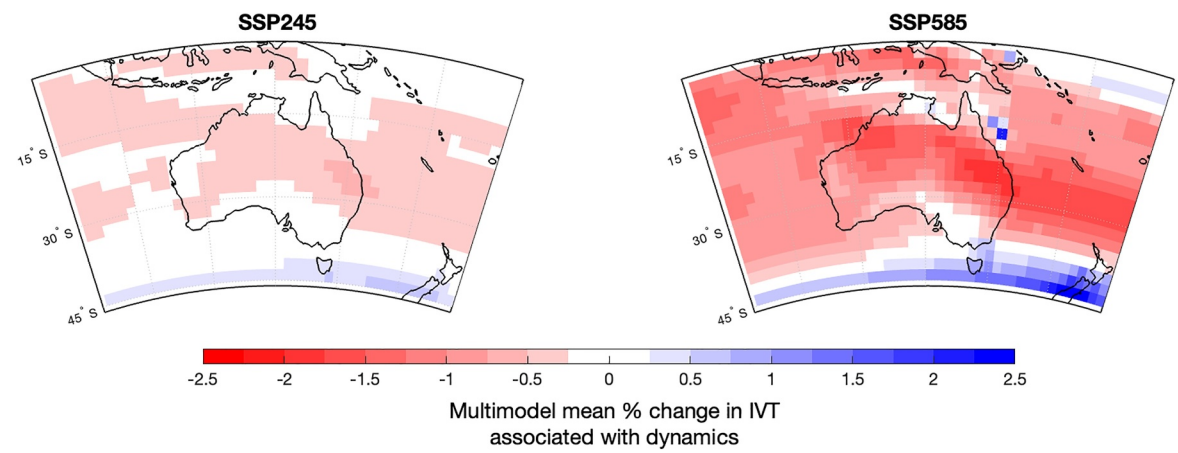

Figure 9. Following the method described in Section 2.2, multimodel mean percentage change in Integrated Water Vapor Transport relative to the historical period (1960–2014) associated with dynamic changes under SSP245 and SSP585.

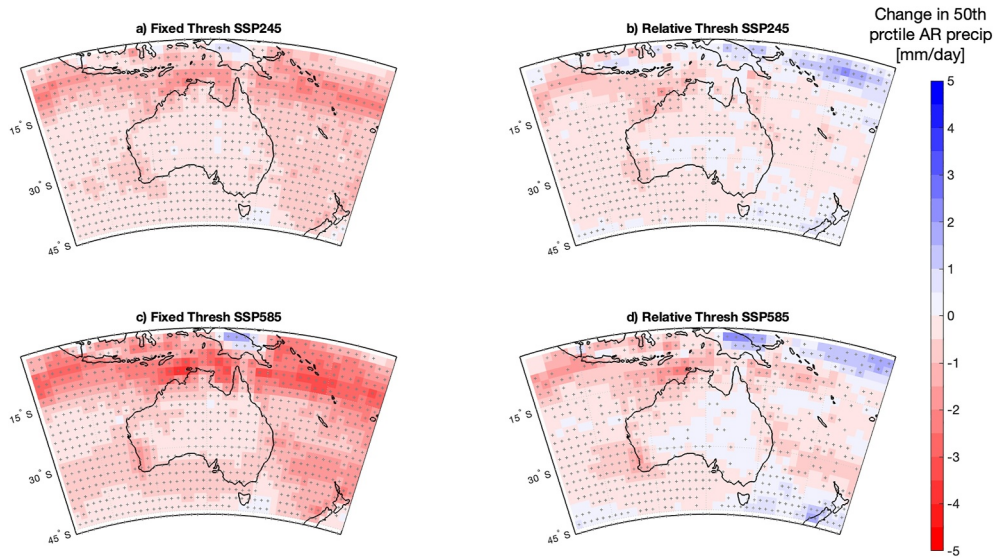

Figure 10. Multimodel mean percentage change in median precipitation associated with atmospheric rivers using (a) fixed thresholding and SSP245, (b) relative thresholding and SSP245, (c) fixed thresholding and SSP585, and (d) relative thresholding and SSP585. Stippling indicates where at least half of the models agree on the sign of the change and the sign is consistent with the multimodel mean. (This same plot for each model under SSP585 are available in Figures S3–S4 in Supporting Information S1).

thermodynamic change in Figure 8 also qualitatively reflects the AR frequency change for the fixed threshold in Figure 6 well. However, the AR frequency change for the relative threshold in Figure 6 is not obviously dominated by thermodynamic or dynamic changes based on this scaling analysis.

Previous work has shown AR detection methods generally show more consensus identifying the core of an AR and more uncertainty around weaker regions such as the boundary of the AR (Lora et al., 2020). Given that precipitation is typically highest where the IVT is highest in the AR core (Reid et al., 2022), we examined how sensitive future AR-associated precipitation projections were to thresholding method. Figure 10 shows the change in the median daily precipitation amount associated with ARs.

Almost all regions show a decrease in median AR precipitation using both thresholding methods and both SSPs. However, there is high uncertainty in the direction of change over southern and eastern Australia using the relative threshold method.

The change in heavy rainfall is more varied (Figure 11). The fixed method leads to uncertain projections for the 95th percentile AR precipitation over most of the continent with a tendency toward decreasing heavy precipitation, whereas the ocean regions appear to experience a decrease in heavy AR precipitation. The relative method suggests that the 95th percentile of AR-associated precipitation will increase over east Australia with more uncertainty in the west. Heavy AR precipitation is projected to increase over northeast Australia using both thresholding methods under SSP585 (Figures 11c and 11d).

Stippling indicates that the increase in 95th percentile AR precipitation is robust over southeast Australia for the relative thresholding method suggesting that the thresholding method rather than model spread is likely causing this difference in sign between the fixed and relative methods over southeast Australia. To understand this difference further, we examined the change in the distribution of daily precipitation intensity for southeast (Figure 12) and southwest (Figure 13) Australia. Daily AR precipitation at each grid within southeast Australia (defined as 41°S to 33°S and 141°E to 151°E longitude) was binned into 0–1, 1–5, 5–10, 10–30, 30–50 and 50 + mm amounts similar to Figure 4 of Shields et al. (2023). We then calculated the change in proportion of days in each of these bins between the future (2080–2100) and historical (1960–2014) period.

For southeast Australia (Figure 12), both thresholding methods project a decrease in the frequency of moderate rain days and an increase in no rain (0–1 mm) and 50 + mm rain days. The frequency change in grids with no rain days is approximately 5–8 times larger when using the fixed threshold compared to the relative threshold, despite

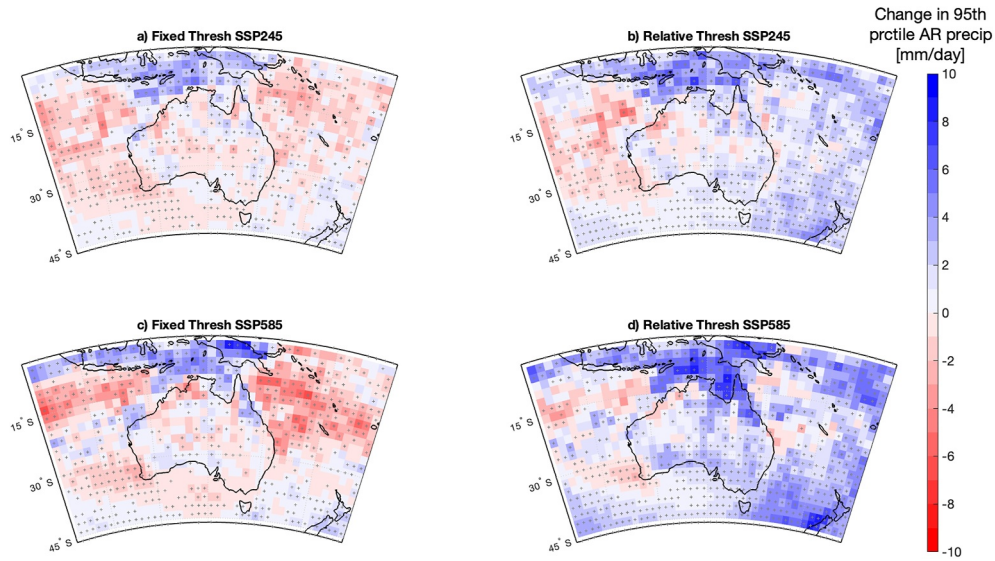

Figure 11. Multimodel mean percentage change in 95th percentile precipitation associated with atmospheric rivers using (a) fixed thresholding and SSP245, (b) relative thresholding and SSP245, (c) fixed thresholding and SSP585, and (d) relative thresholding and SSP585. Stippling indicates where at least half of the models agree on the sign of the change and the sign is consistent with the multimodel mean.

a larger frequency increase in ARs using the fixed method. The increased area of ARs identified with the fixed method (Figure 7) may help to explain why there are more no rain days with this thresholding technique. The additional area classified as an AR by the fixed method would include lower IVT values near the boundary where precipitation is less likely.

The relative method indicates increases in heavy rain days (30 + mm), whereas the fixed method only indicates increases in very heavy rain days (50 + mm), which likely explains why Figure 11 shows increases in the 95th

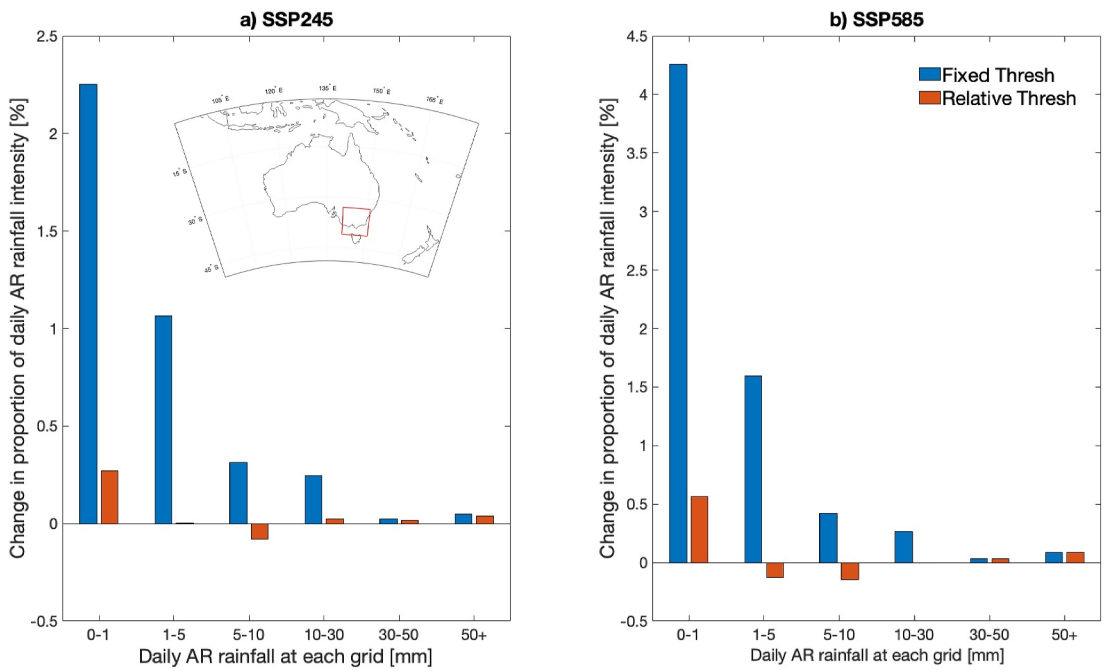

Figure 12. Change in frequency (normalized as a percentage of time) of daily rainfall amounts [mm] for gridboxes in southeast Australia (between 41°S to 33°S and 141°E to 151°E) for the fixed threshold (blue) and relative threshold (orange) under (a) SSP245, and (b) SSP585. Map insert shows the region used.

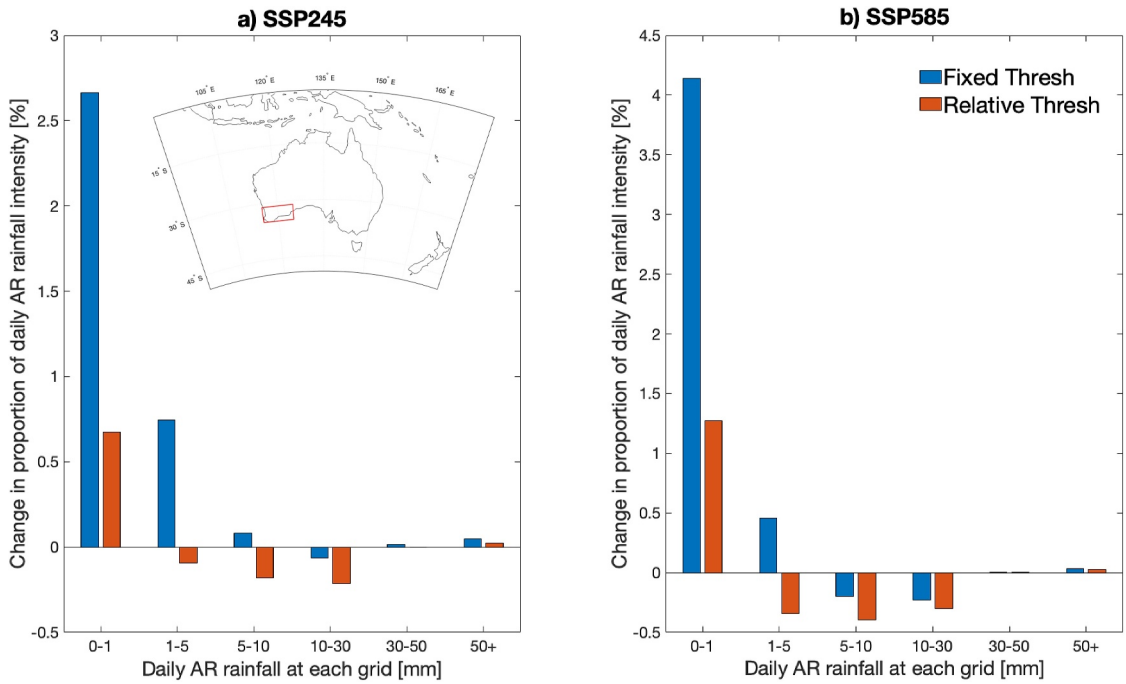

Figure 13. Change in frequency (normalized as a percentage of time) of daily rainfall amounts [mm] for gridboxes in southwest Australia (between 35°S to 31°S and 115°E to 125°E) for the fixed threshold (blue) and relative threshold (orange) under (a) SSP245, and (b) SSP585. Map insert shows the region used.

percentile of AR precipitation in southeast Australia using the relative method but decreases using the fixed method. Despite a minimal change in AR frequency for southeast Australia using the relative method, the AR-associated precipitation distribution does change.

In contrast, both median and 95th percentile rainfall is projected to decrease over southwest Australia (35°S to 31°S and 115°E to 125°E) as shown in Figures 9 and 10. The precipitation intensity distribution in Figure 13 indicates a greater increase in ARs producing 0–1 mm/day (relative to southeast Australia) for both the fixed and relative thresholding methods over southwest Australia. Moreover, the projected AR frequency change does not vary considerably between thresholding methods for southwest Australia (Figure 6). Therefore, the drying in the southwest appears less sensitive to AR identification methods than precipitation changes in southeast Australia. This is not surprising since southwest Australia is one of the few locations with a robust past and future rainfall trend (Dey et al., 2019). However, these results highlight the importance of understanding the sensitivity of rainfall projections to methods in regions without robust trends such as southeast Australia.

6. Atmospheric River Intensity Projections

Finally, we examined the differences in AR intensity using the two thresholding methods. Figure 14 shows how the distribution of mean IVT changes in future projections using the two thresholding methods and two SSPs. The mean IVT (Figure 14a) refers to the areal mean IVT within each AR, whereas the max IVT (Figure 14b) is the maximum IVT at any point within the AR. Below the 90th percentile, the mean IVT within fixed threshold ARs increases uniformly under SSP245 (i.e., the blue dotted line is horizontal for most of the distribution Figure 14a). In contrast, the change in the distribution of mean IVT within relative threshold ARs is more nonlinear. Given relative threshold method ARs are generally smaller than fixed method ARs (Figure 7), we would expect the areal mean IVT to be greater using the relative method. Under SSP585, fixed method ARs (yellow dotted line) have a reduced mean IVT at lower percentiles compared to the historical period. This may be due to disproportionate changes in AR size and intensity when a fixed threshold is used.

We did not expect the maximum IVT within each AR to depend on the size of the AR since the region of maximum IVT within an AR should be encompassed by both IVT thresholding methods. However, Figure 14b indicates some differences in the distribution of maximum IVT between the two thresholding methods. This may

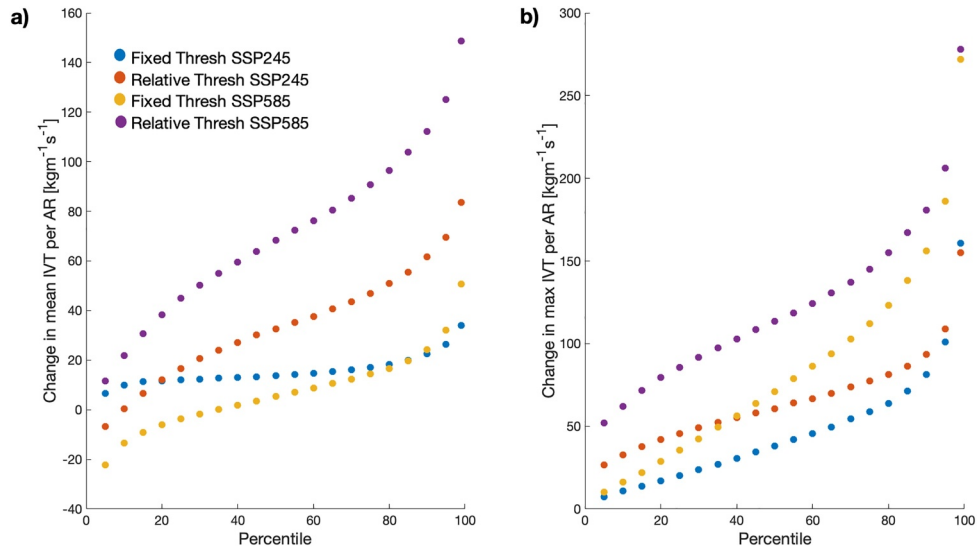

Figure 14. Multimodel mean (mmm) change between historical (1960–2014) and future (2080–2100) periods in the distribution of (a) areal mean Integrated Water Vapor Transport (IVT), and (b) maximum IVT within atmospheric rivers.

be due to a limitation of using geometric requirements in AR identification. Algorithms with less restrictive IVT thresholds may miss the most intense ARs due to identifying rounder ARs that fail the aspect ratio requirement of many AR detection methods (Reid et al., 2020). Beyond the 40th percentile, the change in the distribution of maximum IVT seems to diverge according to SSP rather than thresholding method (Figure 14b). Overall, the relative thresholding method leads to more intense ARs being identified.

7. Discussion and Conclusions

Many weather systems are defined using thresholds. A key challenge with understanding future climate change is determining how to adapt current thresholds that define weather systems or extreme events to a warmer climate (Hobday et al., 2016). Ultimately, there is no perfect method, but there are benefits and limitations for all methods and the choice of method often depends on the application.

In this study we examined the sensitivity of AR frequency and precipitation projections over Australia to the IVT thresholding method. This study addresses two outstanding questions in the literature: (a) how are ARs projected to change over Australia and (b) how sensitive are AR projections to the choice of IVT thresholding method.

The fixed threshold is commonly used in future AR studies (Espinoza et al., 2018; Zhang et al., 2024). This method defines the IVT threshold using the historical climate (i.e., the 85th percentile of IVT over the historical period) and is hence fixed in time. The relative threshold defines the IVT threshold using the climate in which the ARs are being identified (i.e., the 85th percentile of the future period is used when identifying future ARs) and is hence relative in space and time.

However, the two thresholding methods do produce alternative future scenarios, so it is important for researchers and stakeholders to understand which method is being used before drawing conclusions about future projections. Ideally, both methods would be used, and where they agree may indicate a more robust future scenario.

For example, both thresholding methods project an increase (or almost no change) in the frequency of ARs over Australia; however, the extent of the increase in frequency (if any) is sensitive to the IVT thresholding method. It is vital to recognize that an increase in frequency of ARs does not necessarily translate to an increase in AR-associated precipitation. This result is comparable to differences in AR frequency and precipitation between different reanalysis products (Collow et al., 2022). MERRA v2 has higher climatological water vapor than ERA5 and JRA-55, which leads to detection algorithms identifying more ARs, but the mean AR precipitation is lower in MERRA v2 (Collow et al., 2022). The additional frequency of ARs is likely due to weak ARs and hence the AR precipitation does not scale linearly with AR frequency. Similarly, the fixed method likely identifies weaker ARs which do not precipitate as much as intense ARs.

Both thresholding methods lead to an uncertain change or a projected decrease in the median amount of precipitation associated with ARs over Australia which seems to be due to an increase in no rain days (0–1 mm) and a decrease in light—moderate rain days (1–30 mm). The fixed thresholding method suggests a drier future than the relative method. This is likely due to the fixed method identifying more ambiguous and weaker ARs which are associated with less rainfall and therefore may cause an apparent shift in a region's precipitation distribution. In contrast, the relative method identifies more intense ARs and a greater increase in heavy rainfall days associated with ARs over southeast Australia. Both methods suggest an increase in days with 50 + mm associated ARs for southeast Australia. Moreover, both methods indicate a decrease in median and 95th percentile precipitation associated with ARs for southwest Australia. We acknowledge that these conclusions are based on coarse climate model data and higher resolution global climate models are needed to reduce the uncertainty in future precipitation changes.

Additionally, there is considerable model spread in future IVT projections over Australia. Although mean IVT is expected to increase globally (O'Brien et al., 2022), the sign of change is inhomogeneous at the upper end of the distribution. Although internal variability likely dominates 21st century extreme precipitation projections (Blanusa et al., 2023), the role of internal variability in the drivers of precipitation such as IVT has been studied less. Future studies examining IVT in large ensembles would be valuable and examining how different dynamical storylines, such as jet changes and the behavior of annular modes (Baek et al., 2023), may impact IVT and precipitation projections.

The key result of this study is that the choice of method will lead to different conclusions about future projections. End users need to know what method they are basing adaptation decisions off. For more robust conclusions, we recommend researchers employ multiple thresholding methods.

Data Availability Statement

The ERA5 (Hersbach et al., 2020) and CMIP6 (O'Neill et al., 2016) data sets used in this study are publicly available.

The Reid AR identification algorithm (Reid et al., 2020) is available on GitHub-Zenodo: https://doi.org/10.5281/zenodo.15110907.

Acknowledgments
This research was undertaken with the assistance of resources from the National Computational Infrastructure (NCI Australia) supported by the Australian government. The work of Reid was supported by the Australian Research Council Centres of Excellence for Climate Extremes and Weather of the 21st Century (CE170100023 and CE230100012). The work of Allen and Tolgambayev was supported by the Centre of Excellence for Climate Extremes summer internship program. Open access publishing facilitated by The University of Melbourne, as part of the Wiley - The University of Melbourne agreement via the Council of Australian University Librarians.

References

Baek, S. H., Battalio, J. M., & Lora, J. M. (2023). Atmospheric River variability over the last millennium driven by annular modes. *AGU Advances*, *4*(1), e2022AV000834. https://doi.org/10.1029/2022AV000834

Bi, D., Dix, M., Marsland, S., O'Farrell, S., Sullivan, A., Bodman, R., et al. (2020). Configuration and spin-up of ACCESS-CM2, the new generation Australian community climate and earth system simulator coupled model. *Journal of Southern Hemisphere Earth Systems Science*, *70*(1), 225–251. https://doi.org/10.1071/ES19040

Blanusa, M. L., López-Zurita, C. J., & Rasp, S. (2023). Internal variability plays a dominant role in global climate projections of temperature and precipitation extremes. *Climate Dynamics*, *61*(3), 1931–1945. https://doi.org/10.1007/s00382-023-06664-3

Brands, S., Gutiérrez, J. M., & San-Martín, D. (2017). Twentieth-century atmospheric river activity along the west coasts of Europe and North America: Algorithm formulation, reanalysis uncertainty and links to atmospheric circulation patterns. *Climate Dynamics*, *48*(9), 2771–2795. https://doi.org/10.1007/s00382-016-3095-6

Cao, J., Wang, B., Yang, Y. M., Ma, L., Li, J., Sun, B., et al. (2018). The NUIST Earth System Model (NESM) version 3: Description and preliminary evaluation. *Geoscience Model Development*, *11*(7), 2975–2993. https://doi.org/10.5194/gmd-11-2975-2018

Clarke, B., Otto, F., Stuart-Smith, R., & Harrington, L. (2022). Extreme weather impacts of climate change: An attribution perspective. *Environmental Research: Climate*, *1*(1), 012001. https://doi.org/10.1088/2752-5295/ac6e7d

Collow, A. B. M., Shields, C. A., Guan, B., Kim, S., Lora, J. M., McClenny, E. E., et al. (2022). An overview of ARTMIP's tier 2 reanalysis Intercomparison: Uncertainty in the detection of atmospheric rivers and their associated precipitation. *Journal of Geophysical Research: Atmospheres*, *127*(8), e2021JD036155. https://doi.org/10.1029/2021JD036155

Dettinger, M. (2011). Climate change, atmospheric rivers, and floods in California – a multimodel analysis of storm frequency and magnitude changes. *JAWRA Journal of the American Water Resources Association*, *47*(3), 514–523. https://doi.org/10.1111/j.1752-1688.2011.00546.x

Dettinger, M. (2013). Atmospheric rivers as drought busters on the U.S. West coast. *Journal of Hydrometeorology*, *14*(6), 1721–1732. https://doi.org/10.1175/jhm-d-13-02.1

Dey, R., Lewis, S. C., Arblaster, J. M., & Abram, N. J. (2019). A review of past and projected changes in Australia's rainfall. *WIREs Climate Change*, *10*(3), e577. https://doi.org/10.1002/wcc.577

Ebita, A., Kobayashi, S., Ota, Y., Moriya, M., Kumabe, R., Onogi, K., et al. (2011). The Japanese 55-year reanalysis "JRA-55": An interim report. *SOLA*, *7*, 149–152. https://doi.org/10.2151/sola.2011-038

Espinoza, V., Waliser, D. E., Guan, B., Lavers, D. A., & Ralph, F. M. (2018). Global analysis of climate change projection effects on atmospheric rivers. *Geophysical Research Letters*, *45*(9), 4299–4308. https://doi.org/10.1029/2017GL076968

Frederiksen, J. S., & Frederiksen, C. S. (2007). Interdecadal changes in southern hemisphere winter storm track modes. *Tellus A: Dynamic Meteorology and Oceanography*, *59*(5), 599–617. https://doi.org/10.1111/j.1600-0870.2007.00264.x

Gao, Y., Lu, J., Leung, L. R., Yang, Q., Hagos, S., & Qian, Y. (2015). Dynamical and thermodynamical modulations on future changes of landfalling atmospheric rivers over western North America. *Geophysical Research Letters*, *42*(17), 7179–7186. https://doi.org/10.1002/2015GL065435

Gelaro, R., McCarty, W., Suárez, M. J., Todling, R., Molod, A., Takacs, L., et al. (2017). The Modern-Era Retrospective Analysis for Research and Applications, version 2 (MERRA-2). *Journal of Climate*, *30*(14), 5419–5454. https://doi.org/10.1175/jcli-d-16-0758.1

Gershunov, A., Shulgina, T., Ralph, F. M., Lavers, D. A., & Rutz, J. J. (2017). Assessing the climate-scale variability of atmospheric rivers affecting western North America. *Geophysical Research Letters*, *44*(15), 7900–7908. https://doi.org/10.1002/2017GL074175

Grose, M. R., Risbey, J. S., Moise, A. F., Osbrough, S., Heady, C., Wilson, L., & Erwin, T. (2017). Constraints on southern Australian rainfall change based on atmospheric circulation in CMIP5 simulations. *Journal of Climate*, *30*(1), 225–242. https://doi.org/10.1175/jcli-d-16-0142.1

Gutjahr, O., Putrasahan, D., Lohmann, K., Jungclaus, J. H., von Storch, J. S., Brüggemann, N., et al. (2019). Max Planck Institute Earth System Model (MPI-ESM1.2) for the High-Resolution Model Intercomparison Project (HighResMIP). *Geoscience Model Development*, *12*(7), 3241–3281. https://doi.org/10.5194/gmd-12-3241-2019

Held, I. M., & Soden, B. J. (2006). Robust responses of the hydrological cycle to global warming. *Journal of Climate*, *19*(21), 5686–5699. https://doi.org/10.1175/jcli3990.1

Hersbach, H., Bell, B., Berrisford, P., Hirahara, S., Horányi, A., Muñoz-Sabater, J., et al. (2020). The ERA5 global reanalysis. *Quarterly Journal of the Royal Meteorological Society*, *146*(730), 1999–2049. https://doi.org/10.1002/qj.3803

Hobday, A. J., Alexander, L. V., Perkins, S. E., Smale, D. A., Straub, S. C., Oliver, E. C. J., et al. (2016). A hierarchical approach to defining marine heatwaves. *Progress in Oceanography*, *141*, 227–238. https://doi.org/10.1016/j.pocean.2015.12.014

Jin, C., Reeder, M. J., Gallant, A. J. E., Parker, T., & Sprenger, M. (2024). Changes in weather systems during anomalously wet and dry years in southeastern Australia. *Journal of Climate*, *37*(4), 1131–1153. https://doi.org/10.1175/jcli-d-23-0305.1

King, A. D., Reid, K. J., & Saunders, K. R. (2023). Communicating the link between climate change and extreme rain events. *Nature Geoscience*, *16*(7), 552–554. https://doi.org/10.1038/s41561-023-01223-1

Lane, T. P., King, A. D., Perkins-Kirkpatrick, S. E., Pitman, A. J., Alexander, L. V., Arblaster, J. M., et al. (2023). Attribution of extreme events to climate change in the Australian region – a review. *Weather and Climate Extremes*, *42*, 100622. https://doi.org/10.1016/j.wace.2023.100622

Lavers, D. A., Allan, R. P., Villarini, G., Lloyd-Hughes, B., Brayshaw, D. J., & Wade, A. J. (2013). Future changes in atmospheric rivers and their implications for winter flooding in Britain. *Environmental Research Letters*, *8*(3), 034010. https://doi.org/10.1088/1748-9326/8/3/034010

Lavers, D. A., Allan, R. P., Wood, E. F., Villarini, G., Brayshaw, D. J., & Wade, A. J. (2011). Winter floods in Britain are connected to atmospheric rivers. *Geophysical Research Letters*, *38*(23), L23803. https://doi.org/10.1029/2011gl049783

Li, L., Yu, Y., Tang, Y., Lin, P., Xie, J., Song, M., et al. (2020). The Flexible Global Ocean-Atmosphere-Land System model grid-point version 3 (FGOALS-g3): Description and evaluation. *Journal of Advances in Modeling Earth Systems*, *12*(9), e2019MS002012. https://doi.org/10.1029/2019MS002012

Lora, J. M., Shields, C. A., & Rutz, J. J. (2020). Consensus and disagreement in atmospheric river detection: ARTMIP global catalogues. *Geophysical Research Letters*, *47*(20), e2020GL089302. https://doi.org/10.1029/2020GL089302

Lovato, T., Peano, D., Butenschön, M., Materia, S., Iovino, D., Scoccimarro, E., et al. (2022). CMIP6 simulations with the CMCC Earth System Model (CMCC-ESM2). *Journal of Advances in Modeling Earth Systems*, *14*(3), e2021MS002814. https://doi.org/10.1029/2021MS002814

McClenny, E. E., Ullrich, P. A., & Grotjahn, R. (2020). Sensitivity of atmospheric river vapor transport and precipitation to uniform Sea surface temperature increases. *Journal of Geophysical Research: Atmospheres*, *125*(21), e2020JD033421. https://doi.org/10.1029/2020JD033421

McKay, R. C., Boschat, G., Rudeva, I., Pepler, A., Purich, A., Dowdy, A., et al. (2023). Can southern Australian rainfall decline be explained? A review of possible drivers. *WIREs Climate Change*, *14*(2), e820. https://doi.org/10.1002/wcc.820

Muszynski, G., Kashinath, K., Kurlin, V., & Wehner, M., & Prabhat. (2019). Topological data analysis and machine learning for recognizing atmospheric river patterns in large climate datasets. *Geoscience Model Development*, *12*(2), 613–628. https://doi.org/10.5194/gmd-12-613-2019

Neiman, P. J., Ralph, F. M., Wick, G. A., Lundquist, J. D., & Dettinger, M. D. (2008). Meteorological characteristics and overland precipitation impacts of atmospheric rivers affecting the west coast of North America based on eight years of SSM/I satellite observations. *Journal of Hydrometeorology*, *9*(1), 22–47. https://doi.org/10.1175/2007jhm855.1

Nicholls, N., Drosdowsky, W., & Lavery, B. (1997). Australian rainfall variability and change. *Weather*, *52*(3), 66–72. https://doi.org/10.1002/j.1477-8696.1997.tb06274.x

O'Brien, T. A., Wehner, M. F., Payne, A. E., Shields, C. A., Rutz, J. J., Leung, L. R., et al. (2022). Increases in future AR count and size: Overview of the ARTMIP tier 2 CMIP5/6 experiment. *Journal of Geophysical Research: Atmospheres*, *127*(6), e2021JD036013. https://doi.org/10.1029/2021JD036013

O'Neill, B. C., Tebaldi, C., van Vuuren, D. P., Eyring, V., Friedlingstein, P., Hurtt, G., et al. (2016). The Scenario Model Intercomparison Project (ScenarioMIP) for CMIP6. *Geoscience Model Development*, *9*(9), 3461–3482. https://doi.org/10.5194/gmd-9-3461-2016

Parker, T., & Gallant, A. J. E. (2022). The role of heavy rainfall in drought in Australia. *Weather and Climate Extremes*, *38*, 100528. https://doi.org/10.1016/j.wace.2022.100528

Payne, A. E., Demory, M.-E., Leung, L. R., Ramos, A. M., Shields, C. A., Rutz, J. J., et al. (2020). Responses and impacts of atmospheric rivers to climate change. *Nature Reviews Earth and Environment*, *1*(3), 143–157. https://doi.org/10.1038/s43017-020-0030-5

Payne, A. E., & Magnusdottir, G. (2015). An evaluation of atmospheric rivers over the North Pacific in CMIP5 and their response to warming under RCP 8.5. *Journal of Geophysical Research: Atmospheres*, *120*(21), 11173–111190. https://doi.org/10.1002/2015JD023586

Pfahl, S., O'Gorman, P. A., & Fischer, E. M. (2017). Understanding the regional pattern of projected future changes in extreme precipitation. *Nature Climate Change*, *7*(6), 423–427. https://doi.org/10.1038/nclimate3287

Pradhan, S., Wasko, C., & Peel, M. C. (2025). Atmospheric rivers and Australian precipitation: Impact of detection algorithm choice. *Journal of Hydrology*, *651*, 132586. https://doi.org/10.1016/j.jhydrol.2024.132586

Ralph, F. M., Dettinger, M. D., Cairns, M. M., Galarneau, T. J., & Eylander, J. (2018). Defining "atmospheric river": How the glossary of meteorology helped resolve a debate. *Bulletin of the American Meteorological Society*, *99*(4), 837–839. https://doi.org/10.1175/bams-d-17-0157.1

Ralph, F. M., Neiman, P. J., Wick, G. A., Gutman, S. I., Dettinger, M. D., Cayan, D. R., & White, A. B. (2006). Flooding on California's Russian river: Role of atmospheric rivers. *Geophysical Research Letters*, *33*(13), L13801. https://doi.org/10.1029/2006gl026689

Reid, K. J., Hudson, D., King, A. D., Lane, T. P., & Marshall, A. G. (2023). Atmospheric water vapour transport in ACCESS-S2 and the potential for enhancing skill of subseasonal forecasts of precipitation. *Quarterly Journal of the Royal Meteorological Society*, *150*(758), 68–80. n/a(n/a). https://doi.org/10.1002/qj.4585

Reid, K. J., King, A. D., Lane, T. P., & Hudson, D. (2022). Tropical, subtropical, and extratropical atmospheric rivers in the Australian region. *Journal of Climate*, *35*(9), 2697–2708. https://doi.org/10.1175/jcli-d-21-0606.1

Reid, K. J., King, A. D., Lane, T. P., & Short, E. (2020). The sensitivity of atmospheric river identification to integrated water vapor transport threshold, resolution, and regridding method. *Journal of Geophysical Research: Atmospheres*, *125*(20), e2020JD032897. https://doi.org/10.1029/2020JD032897

Reid, K. J., O'Brien, T. A., King, A. D., & Lane, T. P. (2021). Extreme water vapor transport during the march 2021 Sydney floods in the context of climate projections. *Geophysical Research Letters*, *48*(22). https://doi.org/10.1029/2021gl095335

Reid, K. J., Rosier, S. M., Harrington, L. J., King, A. D., & Lane, T. P. (2021). Extreme rainfall in New Zealand and its association with atmospheric rivers. *Environmental Research Letters*, *16*(4), 044012. https://doi.org/10.1088/1748-9326/abeae0

Rudeva, I., Simmonds, I., Crock, D., & Boschat, G. (2019). Midlatitude fronts and variability in the southern hemisphere tropical width. *Journal of Climate*, *32*(23), 8243–8260. https://doi.org/10.1175/jcli-d-18-0782.1

Rutz, J. J., Shields, C. A., Lora, J. M., Payne, A. E., Guan, B., Ullrich, P., et al. (2019). The Atmospheric River Tracking Method Intercomparison Project (ARTMIP): Quantifying uncertainties in atmospheric river climatology. *Journal of Geophysical Research: Atmospheres*, *124*(24), 13777–13802. https://doi.org/10.1029/2019JD030936

Seland, Ø., Bentsen, M., Olivié, D., Toniazzo, T., Gjermundsen, A., Graff, L. S., et al. (2020). Overview of the Norwegian Earth System Model (NorESM2) and key climate response of CMIP6 DECK, historical, and scenario simulations. *Geoscience Model Development*, *13*(12), 6165–6200. https://doi.org/10.5194/gmd-13-6165-2020

Shields, C. A., Payne, A. E., Shearer, E. J., Wehner, M. F., O'Brien, T. A., Rutz, J. J., et al. (2023). Future atmospheric rivers and impacts on precipitation: Overview of the ARTMIP tier 2 high-resolution global warming experiment. *Geophysical Research Letters*, *50*(6), e2022GL102091. https://doi.org/10.1029/2022GL102091

Swapna, P., Roxy, M. K., Aparna, K., Kulkarni, K., Prajeesh, A. G., Ashok, K., et al. (2015). The IITM earth system model: Transformation of a seasonal prediction model to a long-term climate model. *Bulletin of the American Meteorological Society*, *96*(8), 1351–1367. https://doi.org/10.1175/bams-d-13-00276.1

Swart, N. C., Cole, J. N. S., Kharin, V. V., Lazare, M., Scinocca, J. F., Gillett, N. P., et al. (2019). The Canadian Earth system model version 5 (CanESM5.0.3). *Geoscience Model Development*, *12*(11), 4823–4873. https://doi.org/10.5194/gmd-12-4823-2019

Voldoire, A., Saint-Martin, D., Sénési, S., Decharme, B., Alias, A., Chevallier, M., et al. (2019). Evaluation of CMIP6 DECK experiments with CNRM-CM6-1. *Journal of Advances in Modeling Earth Systems*, *11*(7), 2177–2213. https://doi.org/10.1029/2019MS001683

Waliser, D., & Guan, B. (2017). Extreme winds and precipitation during landfall of atmospheric rivers. *Nature Geoscience*, *10*(3), 179–183. https://doi.org/10.1038/ngeo2894

Wu, T., Lu, Y., Fang, Y., Xin, X., Li, L., Li, W., et al. (2019). The Beijing Climate Center Climate System Model (BCC-CSM): The main progress from CMIP5 to CMIP6. *Geoscience Model Development*, *12*(4), 1573–1600. https://doi.org/10.5194/gmd-12-1573-2019

Zhang, L., Zhao, Y., Cheng, T. F., & Lu, M. (2024). Future changes in global atmospheric rivers projected by CMIP6 models. *Journal of Geophysical Research: Atmospheres*, *129*(3), e2023JD039359. https://doi.org/10.1029/2023JD039359

Zhu, Y., & Newell, R. E. (1998). A proposed algorithm for moisture fluxes from atmospheric rivers. *Monthly Weather Review*, *126*(3), 725–735. https://doi.org/10.1175/1520-0493(1998)126<0725:apafmf>2.0.co;2

Ziehn, T., Chamberlain, M. A., Law, R. M., Lenton, A., Bodman, R. W., Dix, M., et al. (2020). The Australian Earth System Model: ACCESS-ESM1.5. *Journal of Southern Hemisphere Earth Systems Science*, *70*(1), 193–214. https://doi.org/10.1071/ES19035